doi:10.14311/ppt.2023.3.127
Plasma Physics and Technology **10**(3):127–131, 2023

CHARACTERIZATION OF ULTRAHIGH PRESSURE NITROGEN ARC USING BLACK BOX ARC MODEL

F. Abid*, K. Niayesh

Department of Electric Energy, Norwegian University of Science and Technology, Trondheim, Norway

* fahim.abid@ntnu.no

Abstract. In this paper, the effect of filling pressure on the black box arc parameters of nitrogen arc is reported using Mayr arc model. The arc current is approximately 130 A at 190 Hz. The filling pressure is varied at absolute pressure of 1, 20, and 40 bar. A phase transition from gas to supercritical state occurs when the pressure of nitrogen exceeds 33.5 bar at room temperature. To determine the effect of forced cooling, first, the free-burning arc is studied at different filling pressures. Afterwards, a self-blast arrangement is used where gas is blown into the arc near current zero. It has been observed that, without forced gas flow, both the time constant and the cooling power of the arc increase with the filling pressure. The forced cooling, however, reduces the time constant and further enhances the cooling power, thus facilitating the current interruption.

Keywords: switchgear, arc discharge, time constant, cooling power, supercritical fluid.

1. Introduction

Offshore substation plays a crucial role in power transmission between offshore installations (e.g., offshore wind farm, offshore mining) and onshore substations. Up to date, mainly two different offshore substation designs exist. One is a conventional floater-based design, where the substation components e.g., switchgear, transformer etc. are placed on a platform. This design requires high installation cost, poses significant challenges in maintenance and is prone to natural calamities. An alternative design approach is to place the substation components directly at seabed in a sealed pressure vessel. The power is fed into the pressure vessel using feedthroughs. Such subsea substation can be controlled remotely and are free from natural disasters [1]. One novel concept to the later design is to gradually fill the pressure vessel with insulating gas to match the surrounding water pressure as the vessel is lowered to seabed. By reducing the differential pressure, the complexity of power cable feedthrough and encapsulations can be reduced.

It is well known that the high gas pressure is associated with improved dielectric performance. A phase transition occurs from gaseous to supercritical (SC) state if the gas pressure and temperature is increased beyond the critical point. In SC state, the properties of gas and liquid coexist. The properties of SC fluid includes improved heat capacity, enhanced dielectric strength, no vapor bubbles, good diffusivity, and self-healing properties [2]. These properties are in line with an excellent current interruption medium. To study the effect of SC fluid on current interruption performance, N_2 is chosen. The critical temperature and pressure are low compared to other insulating gases, i.e., at 126 K and 33.5 bar respectively. This means at a sea depth of approximately 335 m, the N_2 is in SC state. Furthermore, N_2 is an environment friendly gas with good insulating properties.

Gas circuit breakers for medium voltage applications are typically filled at 1.3 bar pressure, while for high voltage (HV) applications the interruption chamber is typically filled up to 6 bar [3]. Hence, the arc characteristics and its switching capability up to several bar filling pressures are well reported in the literature [3, 4]. However, the arc characteristics at very high-pressure gas are limited [2, 5, 6]. Recently, a series of investigations have been carried out to study the ultrahigh pressure N_2 arc and its current interruption capability [7, 8]. The arc voltage is found to rise with filling pressure, thus increasing arc energy deposition [5]. As the pressure is increased, the arc radius reduces [6]. Due to the change in the flow characteristics at high filling pressure and high energy density of the arc column, the thermal phase of the current interruption is observed to be the critical phase for ultrahigh pressure N_2 arc.

Arc interaction with electrical networks can be expressed using black box arc models. The black box models reported in literature mostly follow well known Cassie and Mayr formulations [9]. The Cassie's model is applicable to high current phase while that by Mayr applies to low current regime. This paper employs the Mayr model to investigate how filling pressure influences the arc parameter near current zero (CZ). First, the studies are conducted for free-burning arc, i.e., in the absence of forced cooling. Thereafter, the effect of forced cooling at high filling pressure is investigated using a self-blast principle.

2. Experiment setup

The electrical circuit to initiate the arc is shown in Figure 1. The arc is generated by discharging a charged capacitor bank, C_{bank}. It is charged using a diode rectifier D_{ch} and current limiting resistance, R_{ch}. The

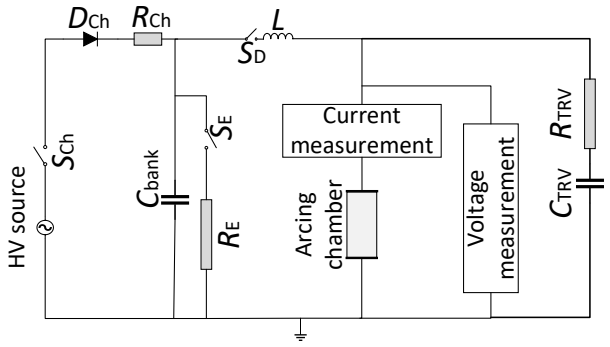

Figure 1. Test circuit.

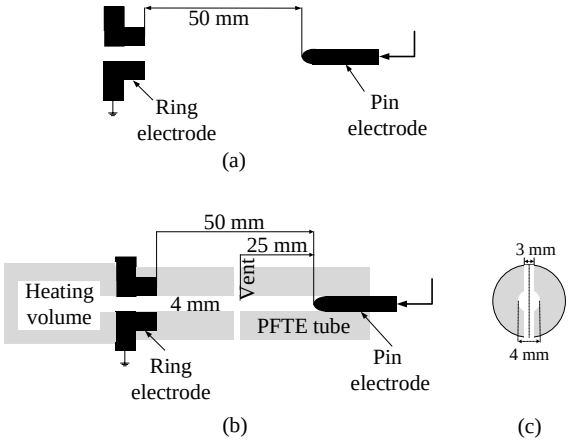

Figure 2. Arc configurations. (a) Free-burning arrangement, (b) Self-blast arrangement, (c) Cross sectional view of the vent for self-blast arrangement.

C_{bank} is separated from the grid by switch S_{ch} once it is charged to the preset level. The C_{bank} is discharged through the inductor, L and thin copper wire inside the arcing chamber by closing the switch S_{D}. The present charging level of C_{bank} is kept fixed. This results in an arc current magnitude of 130 A at a frequency of 190 Hz. As the arc resistance damps the oscillation between the capacitor bank C_{bank} and inductor L. A change in arc voltage slightly influences the arc current and duration of current half cycle. Hence, in this paper, only the first half cycle is investigated for all cases. The shape of recovery voltage is controlled by varying the C_{TRV} and R_{TRV}. In this paper, the steepness of the transient recovery voltage is varied from 9.8 to 84.8 V/µs.

A 15.7 litre pressure vessel is used as the arcing chamber. The arc burns between the arcing contacts, i.e., between pin and ring electrode pair. The arc is initiated by melting of a thin copper ignition wire. First, the free-burning arc is investigated in the absence of forced cooling, as shown schematically in Figure 2(a). The electrode gap is kept constant at 50 mm for both the arcing configurations. A self-blast arrangement is utilized to create gas flow into the arc near CZ. In this arrangement, the arc is confined into PTFE nozzle of 4 mm diameter with vents in the middle, see Figure 2(b). On the other side of the ring electrode, a heating volume is attached. The ablated gas during high current phase is stored in the heating volume. Once the arc current is low, a back-flow of cold gas occurs from the heating volume to the vent of the nozzle. This backflow of gas cools the arc near CZ.

A HV probe is used to measure the arc voltage across the electrodes while the current is measured using a current shunt. The current shunt is placed at the HV side of the arcing contact on a floating potential. The measured data is transferred to the control room using optical fiber link and is stored in a digital oscilloscope.

3. Black box arc model

A black box arc model is a mathematical model that takes its essential characteristics without explicitly modeling the complex physical processes happening in electric arc. It determines the development of arc conductance over time in the form of differential equation. The model is based on the balance between the stored thermal energy in the arc and the cooling of the arc. Two of the most commonly used arc models are Cassie and Mayr arc models. The Mayr arc model is applied for the low-current region close to CZ while the Cassie arc model is applicable to model the high-current region. Often, combined Cassie-Mayr models or modified Mayr models are used to model both the high and low current regions [10]. Nonetheless, Mayr arc model alone is not suitable to study high current arc (i.e., more than several tens of amperes). In Mayr formulations of arc model, the arc radius are assumed to be constant while the temperature of the arc changes. Mayr model is suitable for low current arc, hence, it is used to model current interruption process. The mathematical expression can be written as

$$\frac{1}{g}\frac{\mathrm{d}g}{\mathrm{d}t} = \frac{1}{\tau}\left(\frac{U_{\text{arc}}.I_{\text{arc}}}{P_{\text{o}}}\right) - \frac{1}{\tau} \qquad (1)$$

where the time is defined as t, arc conductance as g, arc voltage as U_{arc}, arc current as I_{arc}, τ as time constant and P_{o} represents the arc cooling power. Although Mayr model is used to study the arc near CZ, due to the presence of noise at very low current, current less than 1 A is not considered. Hence, in this paper, the Mayr arc model is applied for arc current of 10 A and up to 1 A just before CZ.

3.1. Parameter calculation method

First, the high frequency noise from the measured arc voltage and current is removed using first order Savitzky-Golay filter, see Figure 3(a). Afterwards, the arc conductance, g is calculated from the filtered arc voltage and current measurements. As can be seen from Figure 3(a), the conductance, g oscillates as a function of time. This is expected as the effective

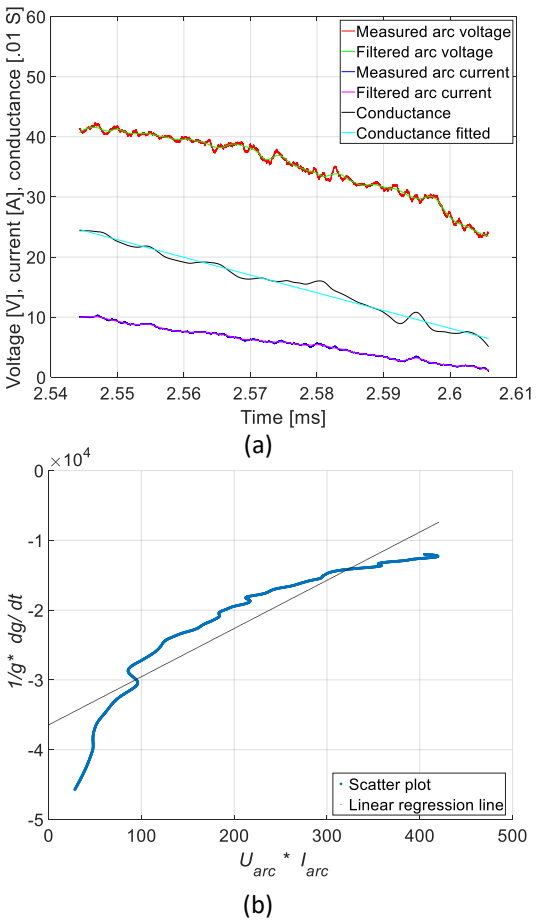

Figure 3. Calculation of arc parameters from measurement of arc voltage and current. (a) Arc voltage, current and conductance. (b) Scatter plot and linear regression line.

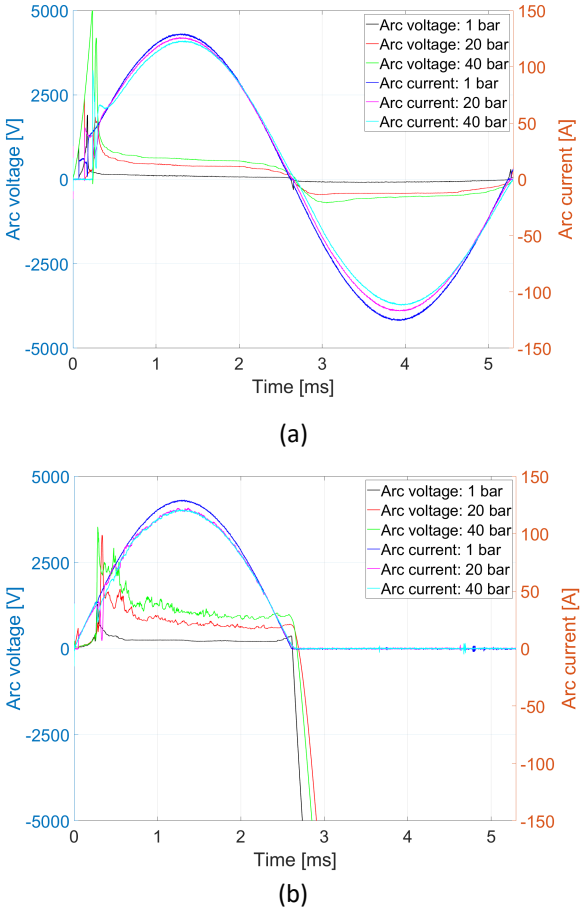

Figure 4. Typical measurement of arc voltage and current at various filling pressures. (a) Free-burning arc, (b) self-blast arrangement.

length of the arc changes over time due to elongation and bending in a three dimensional space. However, in Mayr arc model the arc column is modelled as a cylinder with constant diameter, and hence, the elongation and bending of the arc is not taken into consideration. As such, the conductance, $g(t)$ is fitted to a straight line to calculate the time derivative of the conductance, $\mathrm{d}g/\mathrm{d}t$.

$$\left(\frac{1}{g}\frac{\mathrm{d}g}{\mathrm{d}t}\right) = \frac{1}{\tau P_\mathrm{o}}\left(U_\mathrm{arc}.I_\mathrm{arc}\right) - \frac{1}{\tau} \qquad (2)$$

Equation (1) can be written as equation (2). The left hand side of equation (2) is scatter plotted as a function of the product of arc voltage and current for any specific time, as shown in Figure 3(b). Equation (2) is an equation of a straight line. The intersecting point between the Y-axis and the linear regression line of the scatter plot is the reciprocal of the time constant. Once the time constant is known, the cooling power can be calculated from the slope of the linear regression line, as can be seen from equation (2).

4. Results

A sample measurement of the arc voltage and current for arc burning in various filling pressures at two different arc configurations are plotted in Figure 4. It can be seen that the arc voltage increases with the filling pressure for both configurations. The arc voltages are higher in self-blast arrangement in comparison to free burning arc. Because of the high arc voltage, the current amplitude reduces and time duration for half cycle increases slightly, as seen in Figure 4(a) and Figure 4(b). In the self-blast arrangement, the arc voltage increases just before CZ crossing indicating an extinction peak. In the free-burning arrangement, no such extinction peak is observed.

4.1. Mayr model

The average time constant of the arc with an error bar as a function of filling pressure for both configurations are plotted in Figure 5. Here the error bar represents the maximum and minimum value of the calculated time constant for any specific filling pressure. The time constant of the arc increases with the filling pressure for free-burning arc, as shown in Figure 5(a). The average time constant in free-burning arrange-

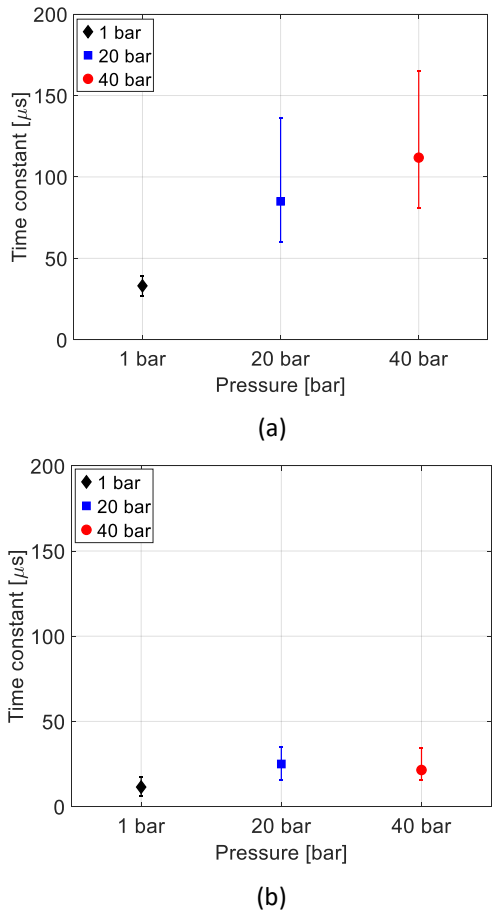

Figure 5. Effect of filling pressure on time constant of the arc. (a) Free-burning arc, (b) self-blast arrangement.

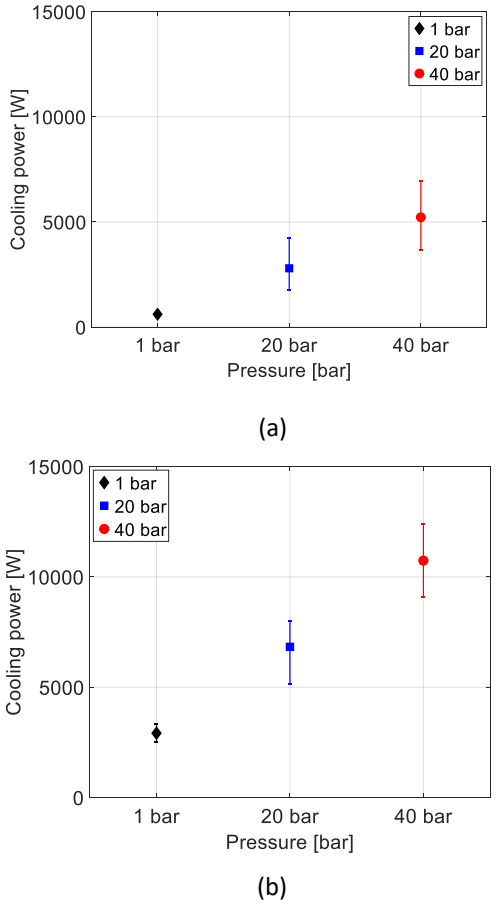

Figure 6. Effect of filling pressure on cooling power of the arc. (a) Free-burning arc, (b) self-blast arrangement.

ment is approximately 33 µs, 86 µs, and 122 µs at 1 bar, 20 bar and 40 bar, respectively. The forced cooling reduces the time constant of the arc when compared to the free-burning arc, as shown in Figure 5(b). In the self-blast arrangement, the average time constant of the arc is found highest at 20 bar filling pressure, i.e., 24 µs whereas the lowest average time constant of approximately 11 µs is found at 1 bar filling pressure.

The calculated average cooling power of the arc as a function of filling pressure is plotted with an error bar in Figure 6. Here the error bar represents the maximum and minimum value of the calculated cooling power for any specific filling pressure. It can be seen that the cooling power of the arc increases with the filling pressure for both free-burning and self-blast arrangement. In free burning arc, the average cooling power is found to be approximately 600 W at 1 bar, as illustrated in Figure 6(a) . The cooling power increases to 2800 W and 5200 W at 20 bar and 40 bar filling pressures, respectively. The cooling power of the arc increases significantly under the influence of forced cooling. In the self-blast arrangement, the average calculated cooling power is approximately 3000 W, 7000 W, and 11000 W at 1 bar, 20 bar and 40 bar filling pressures respectively.

4.2. Current interruption performance

The number of successful current interruption among the tests performed at different filling pressures are listed in Table 1. For free-burning arrangement, the arc fails to interrupt in every first natural CZ irrespective of filling pressures. Under the influence of forced cooling, the 40 bar yields highest interruptions at first CZ, i.e., 20 interruptions out of 30 tests. The current interruption is observed to be lowest at 20 bar filling pressure, i.e., 9 interruptions out of 30 experiments.

The arc temperature varies at different filling pressures for different arc configurations. Furthermore, the material property of the gas changes with the filling pressure. If the temperature of the arc near CZ is such that the thermal conductivity is low, then the cooling will be affected. Moreover, a high pressure is associated with higher viscosity which may shift the flow characteristics from turbulent to more laminar flow. It is observed that the cooling power of the arc increases with the filling pressure. The calculated average time constant of the arc in self-blast arrangement is observed to be highest in 20 bar, see Figure 5(b).

Pressure [bar]	Free-burning	Self-blast
1	0/30	16/30
20	0/30	9/30
40	0/30	20/30

Table 1. Rate of successful arc interruption as a function of filling pressure.

A higher time constant of the arc is often associated with reduced interruption capability. As such, the reduced thermal conductivity and change in flow characteristics resulting in relatively high time constant may adversely affect the interruption performance at 20 bar for the tested nozzle arrangement.

5. Conclusions

Effect of filling pressure on the black box arc parameters for nitrogen arc is investigated in this paper. Two different arc configurations are studied: free-burning arc (without forced cooling) and using a self-blast arrangement (with forced cooling). To investigate the arc behaviour at low current, Mayr arc model is used. On the basis of the results, following conclusions have been drawn:

1. The cooling power of the arc increases with the filling pressure in both the free-burning and self-blast arc arrangements. The forced gas flow further improves the cooling power.

2. The time constant of the arc typically increases with the filling pressure in both the configurations. The forced gas flow from self-blast arrangement reduces the time constant.

Acknowledgements

Support from Norwegian Research Council through project 280539 is highly appreciated. The authors would like to thank Dr. Nina Sasaki Støa-Aanensen for her help throughout the project.

References

[1] T. Hazel, H. H. Baerd, J. J. Legeay, and J. J. Bremnes. Taking power distribution under the sea: Design, manufacture, and assembly of a subsea electrical distribution system. *IEEE Industry Applications Magazine*, 19(5):58–67, 2013. doi:10.1109/MIAS.2012.2215648.

[2] J. Zhang, A. H. Markosyan, M. Seeger, et al. Numerical and experimental investigation of dielectric recovery in supercritical N_2. *Plasma Sources Science and Technology*, 24(2), 2015. doi:10.1088/0963-0252/24/2/025008.

[3] Z. Guo, S. Liu, Y. Pu, et al. Study of the arc interruption performance of CO_2 gas in high-voltage circuit breaker. *IEEE Transactions on Plasma Science*, 47(5):2742–2751, 2019. doi:10.1109/TPS.2019.2904981.

[4] M. Seeger, M. Schwinne, R. Bini, et al. Dielectric recovery in a high-voltage circuit breaker in SF_6. *Journal of Physics D: Applied Physics*, 45(5), 2012. doi:10.1088/0022-3727/45/39/395204.

[5] F. Abid, K. Niayesh, E. Jonsson, et al. Arc voltage characteristics in ultrahigh-pressure nitrogen including supercritical region. *IEEE Transactions on Plasma Science*, 46(1):187–193, 2018. doi:10.1109/TPS.2017.2778800.

[6] F. Abid, K. Niayesh, C. Espedal, and N. S. Støa-Aanensen. Current interruption performance of ultrahigh-pressure nitrogen arc. *Journal of Physics D: Applied Physics*, 53(18):185503, 2020. doi:10.1088/1361-6463/ab7352.

[7] F. Abid, K. Niayesh, E. Viken, et al. Effect of filling pressure on post-arc gap recovery of N_2. *IEEE Transactions on Dielectrics and Electrical Insulation*, 27(4):1339–1347, 2020. doi:10.1109/TDEI.2020.008844.

[8] A. Kadivar, K. Niayesh, N. S. Støa-Aanensen, and F. Abid. Metal vapor content of an electric arc initiated by exploding wire in a model n_2 circuit breaker: Simulation and experiment. *Journal of Physics D: Applied Physics*, 54(5), 2012. doi:10.1088/1361-6463/abba92.

[9] J. L. Guardado, S. G. Maximov, E. Melgoza, et al. An improved arc model before current zero based on the combined mayr and cassie arc models. *IEEE Transactions on Power Delivery*, 20(1), 2005. doi:10.1109/TPWRD.2004.837814.

[10] A. Khakpour, S. Franke, S. Gortschakow, et al. An improved arc model based on the arc diameter. *IEEE Transactions on Power Delivery*, 31(3), 2016. doi:10.1109/TPWRD.2015.2473677.